Plant, Cell & Environment

Plant, Cell and Environment (2014) **37**, 1989–2001 doi: 10.1111/pce.12335

Original Article

Expanding knowledge of the Rubisco kinetics variability in plant species: environmental and evolutionary trends

Jeroni Galmés[1], Maxim V. Kapralov[2], P. John Andralojc[3], Miquel À. Conesa[1], Alfred J. Keys[3], Martin A. J. Parry[3] & Jaume Flexas[1]

[1]Research Group on Plant Biology under Mediterranean Conditions, Universitat de les Illes Balears, Palma, Spain, [2]Plant Science Division, Research School of Biology, The Australian National University, Canberra, Australian Capital Territory 0200, Australia and [3]Plant Biology and Crop Science, Rothamsted Research, Harpenden AL5 2JQ, UK

ABSTRACT

The present study characterizes the kinetic properties of ribulose-1,5-bisphosphate carboxylase/oxygenase (Rubisco) from 28 terrestrial plant species, representing different phylogenetic lineages, environmental adaptations and photosynthetic mechanisms. Our findings confirm that past atmospheric CO_2/O_2 ratio changes and present environmental pressures have influenced Rubisco kinetics. One evolutionary adaptation to a decreasing atmospheric CO_2/O_2 ratio has been an increase in the affinity of Rubisco for CO_2 (K_c falling), and a consequent decrease in the velocity of carboxylation (k_{cat}^c), which in turn has been ameliorated by an increase in the proportion of leaf protein accounted by Rubisco. The trade-off between K_c and k_{cat}^c was not universal among the species studied and deviations from this relationship occur in extant forms of Rubisco. In species adapted to particular environments, including carnivorous plants, crassulacean acid metabolism species and C_3 plants from aquatic and arid habitats, Rubisco has evolved towards increased efficiency, as demonstrated by a higher k_{cat}^c/K_c ratio. This variability in kinetics was related to the amino acid sequence of the Rubisco large subunit. Phylogenetic analysis identified 13 residues under positive selection during evolution towards specific Rubisco kinetic parameters. This crucial information provides candidate amino acid replacements, which could be implemented to optimize crop photosynthesis under a range of environmental conditions.

Key-words: evolution; photosynthesis; stress.

INTRODUCTION

In spite of the pivotal role of the enzyme ribulose-1,5-bisphosphate carboxylase/oxygenase (Rubisco) in determining photosynthetic capacity, this enzyme manifests important catalytic inefficiencies arising from slow turnover and poor discrimination between CO_2 and O_2 (Tcherkez *et al*. 2006). Reaction with O_2 instead of CO_2 leads to photorespiration and the consequent loss of fixed carbon, nitrogen and energy (Keys 1986). To compensate for these inadequacies, plants frequently possess very large amounts of Rubisco, although this almost certainly has negative consequences for nitrogen use efficiency.

All present-day forms of Rubisco are descendants of an ancestral protein, which evolved approximately 3 billion years ago in bacteria inhabiting the anoxic ocean (Badger & Andrews 1987; Nisbet *et al*. 2007; Whitney *et al*. 2011a). Operation of the carboxylase activity of Rubisco within the reductive pentose phosphate (Calvin–Benson–Bassham) cycle together with carboxylase activity of enzymes from other autotrophic inorganic carbon assimilation pathways (e.g. 3-hydroxypropionate CO_2 fixation cycle; Zarzycki *et al*. 2009) coupled with the geological long-term burial of organic carbon have led to removal of a significant proportion of carbon dioxide from the atmosphere-ocean system over geological time scales. In parallel with this, atmospheric O_2 was increasing as a result of the activities of aquatic oxygenic phototrophs, causing the oxygenation of the atmosphere between 2.3 and 0.5 billion years ago, which has increasingly favoured oxygenation (and consequently photorespiration) over carboxylation (Nisbet *et al*. 2007). Therefore, progressive evolutionary adaptation of the catalytic mechanism of Rubisco in response to the gradual change in $[CO_2]$ and $[O_2]$ has been necessary to optimize CO_2 specificity to the CO_2 concentration around its active sites (Nisbet *et al*. 2007). This hypothesis is supported by the timing of positive selection events acting on Rubisco, which coincides with changes in the atmospheric $[CO_2]/[O_2]$ ratio (Young *et al*. 2012). Additional support comes from the theoretical analysis of carbon uptake at the leaf (Galmés *et al*. 2014) and canopy level (Zhu *et al*. 2004) that suggests that the average kinetics of Rubisco in modern C_3 plants reflects the trade-off between K_c and k_{cat}^c and is optimized for the average atmospheric CO_2 concentration of the past 400 000 years, of around 200 ppm. Rubisco of land plants has undergone more extensive positive selection than that of algae, perhaps as a consequence of land colonization involving diversification into numerous ecological niches (Kapralov & Filatov 2007). As a result of this selection pressure, considerable variation exists in the catalytic properties of Rubisco both among distant phylogenetic groups (Jordan & Ogren 1981; Keys 1986; Kent & Tomany 1995; Uemura

Correspondence: J. Galmés. Fax: +34 9711 73168; e-mail: jeroni.galmes@uib.cat

et al. 1997; Badger *et al*. 1998; Whitney & Andrews 1998; Tabita 1999; Raven 2000; Tcherkez *et al*. 2006; Andersson & Backlund 2008; Savir *et al*. 2010; Whitney *et al*. 2011a) and within closely related taxa (Yeoh *et al*. 1980, 1981; Galmés *et al*. 2005; Kubien *et al*. 2008; Ishikawa *et al*. 2009).

Accessibility of CO_2 to the active sites of Rubisco is one of the major factors driving changes in the kinetics of Rubisco in terrestrial species (Delgado *et al*. 1995; Raven 2000; Savir *et al*. 2010). Thus, plants possessing the C_4 carbon concentration mechanism have faster, but less CO_2 specific Rubisco (Yeoh *et al*. 1980, 1981; Seemann *et al*. 1984; Ghannoum *et al*. 2005; Kubien *et al*. 2008; Carmo-Silva *et al*. 2010). In contrast, Rubisco from species adapted to dry, warm and saline habitats have correspondingly adapted to the relatively low CO_2 concentrations caused by decreased leaf conductance – which hampers the transfer of atmospheric CO_2 to the chloroplast stroma (Galmés *et al*. 2005, 2011).

Universal structural constraints dictate that changes in the affinity of Rubisco for CO_2 (i.e. the inverse of the Michaelis–Menten constant for CO_2, K_c) are negatively correlated to the maximum rate of carboxylation (k_{cat}^c). In spite of this trade-off between k_{cat}^c and affinity for CO_2, published data reveal significant variability in the carboxylase catalytic efficiency (k_{cat}^c/K_c; Tcherkez *et al*. 2006; Savir *et al*. 2010; Whitney *et al*. 2011a). Knowledge of the relationships between – and the permissible combinations of – Rubisco kinetic parameters is limited by the number of species for which kinetics have been characterized. To date, Rubisco catalytic parameters have been determined for less than 0.025% of land plants (Badger *et al*. 1998; Savir *et al*. 2010; Whitney *et al*. 2011a). Moreover, most of this limited characterization of Rubisco kinetics has been performed at 25 °C, and conclusions may vary if comparisons are made at different temperatures (Walker *et al*. 2013). This lack of information constrains the knowledge of Rubisco evolution and of the true diversity of Rubisco kinetic characteristics.

The accuracy of all mechanistic models to predict leaf carbon fixation depend on the kinetic properties of Rubisco (Farquhar *et al*. 1980; Von Caemmerer 2000). Although photosynthesis models are frequently applied assuming identical kinetic parameters among species (e.g. Niinemets *et al*. 2009; von Caemmerer, 2013), when the effect of small improvements to its kinetic properties are incorporated, increases in net photosynthesis of up to 60% have been predicted (Reynolds *et al*. 2009; Zhu *et al*. 2010). Recent theoretical advances in the modelling of leaf gas exchange, together with technical advances in plastome transformation, have rekindled the expectation that improvements in the catalytic properties of Rubisco can be introduced into crop species, and that this in turn will facilitate an increase in photosynthetic capacity (Sharwood *et al*. 2008; Ishikawa *et al*. 2011; Whitney *et al*. 2011b). The success of Rubisco bioengineering approaches could be facilitated both by the discovery of more efficient extant forms of Rubisco and by a greater understanding of the identity and role of pivotal amino acid residues within this enzyme. Studies of the natural variation in the chloroplast gene *rbc*L, which encodes Rubisco large subunits (L-subunits), within a phylogenetic framework have led to the identification of candidate amino acid substitutions responsible for altered kinetic characteristics (Kapralov & Filatov 2007; Christin *et al*. 2008; Kapralov *et al*. 2011, 2012) as well as widespread co-evolution between residues (Wang *et al*. 2011). One of these amino acid replacements has been tested *in planta* and has proved to significantly increase the velocity of carboxylation (Whitney *et al*. 2011b), confirming the predictions made *in silico* (Kapralov *et al*. 2011) and justifying optimism for future Rubisco improvement in crops.

The present study characterizes key Rubisco kinetic parameters and the corresponding chloroplast *rbc*L gene sequences in 28 plant species, representing different phylogenetic and ecological groups, including several cultivars of two crop species. The main objectives of the study were (1) to broaden our knowledge of the evolution and natural variability of Rubisco kinetics in C_3 species and in plants with carbon concentrating mechanisms; (2) to test for the presence of kinetic variation within the same crop species; (3) to relate Rubisco kinetic variability to the evolution of Rubisco under different environmental pressures; and (4) to identify candidate amino acid substitutions responsible for the observed kinetic variability.

MATERIALS AND METHODS

Species selection and sampling

Twenty-eight species of land plants including bryophytes (*Atrichum undulatum* (Hedw.) P. Beauv and *Marchantia polymorpha* L.), ferns (*Platycerium superbum* Jonch. & Hennipman and *Pteridium aquilinum* (L.) Kuhn), gymnosperms (*Cycas panzhihuaensis* L. Zhou & S.Y. Yang and *Metasequoia glyptostroboides* Hu & W.C. Cheng) and angiosperms (22 species; Table 1) were selected to represent contrasting and previously neglected groups. Angiosperms were divided into the basal angiosperm (*Nymphaea alba* L.), which originated in the CO_2-rich atmosphere of the earliest Cretaceous (Friis *et al*. 2001), and species of more recent origin (Mesangiospermae). The latter group was subdivided according to species ecology and the presence/absence of CO_2 concentrating mechanisms (CCMs) into submerged aquatic macrophytes utilizing HCO_3^- (*Ceratophyllum demersum* L.; Van *et al*. 1976); crassulacean acid metabolism (CAM) species (*Agave victoriae-reginae* T. Moore, *Carpobrotus edulis* (L.) N.E. Br. and *Echeveria elegans* Rose); carnivorous plants from nitrogen- and phosphorous-deficient habitats (*Drosera venusta* Debbert, *D. capensis* L. and *Sarracenia flava* L.); C_3 plants from low stress environments (*Arabidopsis thaliana* (L.) Heynh., *Dactylis glomerata* L., *Eucalyptus moorei* Maiden & Cambage, *E. neglecta* Maiden, *Iris douglasiana* Herb., *Trachycarpus fortunei* (Hook.) H. Wendl. and *Triticum aestivum* L.); and C_3 plants from environments with high osmotic and heat stress (*Limonium latebracteatum* Erben, *L. stenophyllum* Erben, *L. virgatum* (Willd.) Fourr., *Pallenis maritima* (L.) Greuter, *Crithmum maritimum* L., *Sideritis cretica* subsp. *spicata*

(Pit.) Marrero Rodr. and *Teucrium heterophyllum* L'Hér.). In addition, by way of screening for intraspecific variability, five wheat genotypes (*Triticum aestivum* cv. Alexandria, plus four Mexican genotypes selected under drought stress) and three *Dactylis glomerata* cultivars (Jana, Kasbah and Porto) were included in the study.

Three to six individuals of each species were grown in a glasshouse at Rothamsted Research, Harpenden, UK, with the exceptions of *N. alba* and *C. demersum*, which were collected fresh from a pond close to Rothamsted Research. The glasshouse conditions were a photoperiod of 16 h with minimum temperatures of 25 °C and 18 °C during the light and dark periods, respectively. Plants were grown in soil-based compost supplemented with slow-release fertilizer (except the carnivorous species) and watered sparingly by hand.

Rubisco extraction

0.5 g fresh weight of photosynthetic organs (young leaves and/or green stems) were sampled in full sunlight, immediately frozen in liquid nitrogen and ground in a mortar with 2 mL of ice-cold extraction buffer containing 100 mM Bicine (pH 8.2), 6% (w/v) PEG 4000, 2 mM $MgCl_2$, 0.1 mM ethylenediaminetetraacetic acid (EDTA), 1 mM benzamidine, 1 mM ε-aminocaproic acid, 50 mM 2-mercaptoethanol, 10 mM Dithiothreiol (DTT), 2 μM pepstain A, 10 μM E64, 10 μM chymostatin, 2 mM phenylmethylsulphonylfluoride (PMSF) and 2.5% (w/v) polyvinylpolypyrrolidone (PVPP). The liquidized homogenate was clarified by centrifugation at 12 842 *g* during 4 min at 4 °C. 1 mL of the supernatant was applied to a Sephadex G-25 (PD-10) column (GE Healthcare, UK) pre-equilibrated with desalt buffer, containing 100 mM Bicine (pH 8.2), 20 mM $MgCl_2$, 10 mM DTT, 1 mM KH_2Pi, 0.5 mM EDTA, 1 mM benzamidine, 1 mM ε-aminocaproic acid and 10 mM $NaHCO_3$. The protein peak (in 1 mL) was supplemented with protease inhibitors (4 μM pepstain A, 20 μM E64 and 20 μM chymostatin) and 250 μL of this mixture was supplemented with sufficient carrier-free $NaH^{14}CO_3$ to adjust the specific radioactivity to 3.7×10^{10} Bq mol^{-1}. The remaining extract was frozen immediately in liquid nitrogen for the measurement of Rubisco active site concentration (Yokota & Canvin 1985).

CAM plants did not show sufficient enzyme activity when extracted as above, but produced active enzyme when the concentration of Bicine in the extraction buffer was increased to 500 mM.

Rubisco kinetic characterization

Preliminary tests performed on four contrasting species showed that maximum carboxylase activities were obtained 30 to 45 min after protein elution from the Sephadex columns (in a buffer designed to facilitate full Rubisco activation), after which it steadily declined during the ensuing 30 min. Therefore, the Rubisco kinetic assays were started 30 min after elution from the Sephadex columns, and were completed within 15 min.

Rates of Rubisco $^{14}CO_2$-fixation using the activated protein extract were measured at 25 °C in 7 mL septum capped scintillation vials, containing reaction buffer (yielding final concentrations of 100 mM Bicine-NaOH pH 8.0, 20 mM $MgCl_2$, 0.4 mM RuBP and about 100 W-A units of carbonic anhydrase) equilibrated either with nitrogen (N_2) or a mixture of O_2 and N_2 (45:55) and containing nine different concentrations of $^{14}CO_2$ (0 to 80 μM, each with a specific radioactivity of 3.7×10^{10} Bq mol^{-1}), as described previously (Parry *et al*. 2007). Assays (1.0 mL total volume) were started by prompt addition of 25 or 50 μL of activated leaf extract and quenched after 1 min by the addition of 0.1 mL of 10 M formic acid. Acid-stable ^{14}C was determined by liquid scintillation counting, following removal of acid-labile ^{14}C by evaporation. The Michaelis–Menten constant (K_M) for CO_2 (K_c) was determined from the fitted data as described elsewhere (Bird *et al*. 1982). The K_M for O_2 (K_o) was calculated from the relationship $K_{c,(45\%O2)} = K_{c,(0\%O2)} \cdot (1 + [O_2]/K_o)$. The concentration of O_2 in the assay media was calculated assuming the solubility at a partial pressure equivalent to one standard atmosphere (101.325 kPa) to be 265 μM at 25 °C, and correcting for actual partial pressure of O_2 by taking account of the prevailing atmospheric pressure and saturated water vapour pressure at 25 °C (Erlich Industrial Development Corp. – http://www.eidusa.com/Theory_DO.htm). Replicate measurements ($n = 3$) were made using independent protein preparations from different individuals. For each sample, the maximum rate of carboxylation (k_{cat}^c) was extrapolated from the Michaelis–Menten fit and then normalized by dividing the rate by the number of Rubisco active sites, quantified by [^{14}C]CABP binding (Yokota & Canvin 1985).

We have consistently found that the highest estimates for Rubisco catalytic activity are obtained using rapidly extracted leaf-soluble protein. Attempts to further purify the enzyme prior to assay frequently leads to loss of catalytic activity, causing underestimation of the catalytic potential of Rubisco. Such preparations are necessarily crude, necessitating additional controls to establish that the observed acid stable ^{14}C is the result of Rubisco catalytic activity. Thus, similar assays to those described above with a constant $^{14}CO_2$ concentration of 100 μM (1.85×10^{10} Bq mol^{-1}) were routinely performed, in duplicate, in the presence and absence of either 0.4 mM RuBP (to establish the RuBP dependence of ^{14}C fixation) or 40 μM 3-phosphoglycerate (to test for ^{14}C fixation arising from the products of Rubisco carboxylase activity) together with the same Rubisco preparation as used in the kinetic assays, both before and after CABP inhibition (to further demonstrate the Rubisco dependence of $^{14}CO_2$ assimilation). None of the species tested showed signs of competing activities (results not shown).

DNA extraction and *rbc*L sequencing

Leaf tissue from a single individual of each species or genotype/cultivar (in the case of *T. aestivum and*

D. glomerata) was sampled and frozen in liquid nitrogen. Genomic DNA was extracted from the powdered tissue using DNeasy Plant Mini Kit (Qiagen, Hilden, Germany) according to the manufacturer's protocol. The chloroplast gene *rbc*L, which encodes the large subunit of Rubisco, was amplified and sequenced using primers described (Savolainen *et al*. 2000; Cuénoud *et al*. 2002; Tamura *et al*. 2004; Masuzaki *et al*. 2010) for all species with exception of two eucalypts (*E. moorei* and *E. neglecta*), which were substituted in the further phylogenetic analysis by the *rbc*L sequences from the related species, *E. grandis* W. Hill and *E. globulus* Labill., obtained from GenBank. For PCR amplification the BioMix Red (Bioline, London, UK) was used with the following PCR conditions: one cycle of 95 °C, 2 min, 55 °C, 30 s, 72 °C, 4 min followed by 36 cycles of 93 °C, 30 s, 53 °C, 30 s, 72 °C, 3.5 min. The PCR products were extracted from the agarose gels using the Qiagen gel extraction kit. Sequencing was performed using ABI BigDye v3.1 system on an ABI3700 automated sequencing machine. Novel sequences have been submitted to GenBank under accession numbers AB917041-AB917066.

Statistical analyses

Univariate analysis of variance (ANOVA) was used to compare the different kinetic parameters among species/cultivar or groups of species. Significant differences between means were revealed by Duncan test ($P < 0.05$). These analyses were performed using the SPSS 12.0 software package (SPSS Inc., Chicago, IL, USA).

Pearson's correlations were calculated for all pairwise combinations of traits. However, correlations arising within groups of related taxa might reflect phylogenetic signal rather than true cause–effect relationships because closely related taxa are not necessarily independent data points thus violating the assumption of randomized sampling employed by conventional statistical methods (Felsenstein 1985). To overcome this issue, tests were performed for the presence of phylogenetic signal in the data and trait correlations were calculated with independent contrasts using the AOT module of PHYLOCOM (Webb *et al*. 2008). All these tests were considered significant at $P < 0.05$. All trait data were log10-transformed prior to contrast calculation. Phylogenetically independent contrasts (PICs) for all functional traits were calculated using the derived reference phylogeny for the 28 species used in these analyses. The maximum likelihood phylogeny was reconstructed using only synonymous positions of the *rbc*L alignment to avoid potential distortion caused by non-synonymous sites under positive selection (Kapralov & Filatov 2007). Although *T. aestivum* and *D. glomerata* were represented by several cultivars, the *rbc*L sequences within each species were identical. Hence, we used the tree containing only 28 unique species where *T. aestivum* and *D. glomerata* were represented by *T. aestivum* cv. Alexandria and *D. glomerata* cv. Porto, respectively (Supporting Information Fig. S1).

Analysis of Rubisco L-subunit sites under positive selection

Amino acid residues under positive selection have been identified using codon-based substitution models in comparative analysis of protein-coding DNA sequences within the phylogenetic framework (Yang 1997). Given the conservative assumption of no selective pressure at synonymous sites, codon-based substitution models assume that codons with the ratio of nonsynonymous/synonymous substitution rate $d_N/d_S < 1$ evolve under purifying selection to keep protein function and properties, while codons with $d_N/d_S > 1$ evolve under positive Darwinian selection to adapt/change properties of the given protein (Yang 1997).

The codeml program in the PAML v.4.4 package (Yang 2007) was used to perform branch-site tests of positive selection along pre-specified foreground branches (Yang *et al*. 2005; Yang 2007). The codeml A model allows $0 \le d_N/d_S \le 1$ and $d_N/d_S = 1$ for all branches, and also two classes of codons under positive selection with $d_N/d_S > 1$ along pre-specified foreground branches while restricting as $0 \le d_N/d_S \le 1$ and $d_N/d_S = 1$ on background branches. In six independent tests branches leading to species with high or low K_c, k_{cat}^c and K_o were marked as foreground branches. For the purpose of these tests, high or low K_c, k_{cat}^c and K_o were taken as $K_c \le 9.0\ \mu M$ and $K_c \ge 11.0\ \mu M$, $k_{cat}^c \le 3.0\ s^{-1}$ and $k_{cat}^c \ge 4.0$ and $K_o \le 400.0\ \mu M$ and $K_o \ge 500.0\ \mu M$, respectively. To identify amino acid sites potentially under positive selection, the parameter estimates from the A model were used to calculate the posterior probabilities that an amino acid belongs to a class with $d_N/d_S > 1$ using the Bayes empirical Bayes (BEB) approach implemented in PAML (Yang *et al*. 2005).

For the analysis of Rubisco sites under positive selection, we used the published Rubisco protein structure from spinach (*Spinacia oleracea* L., Amaranthaceae) obtained from the RCSB Protein Data Bank (http://www.rcsb.org; file 1UPM; Karkehabadi *et al*. 2003). Throughout the paper, the numbering of Rubisco L-subunit residues is based on the spinach sequence. The locations of individual amino acids in the Rubisco structure were analysed using DeepView – Swiss-PdbViewer v.3.7 (Kaplan & Littlejohn 2001).

RESULTS

Variability of Rubisco kinetics

With 28 different species, the present study provides one of the largest datasets of the kinetic properties of Rubisco. The affinity of Rubisco for CO_2 measured as K_c varied between 6.4 μM (the Mediterranean angiosperm *Pallenis maritima* from high osmotic and heat stress environments) and 19.2 μM (the moss *Atrichum undulatum*; Table 1). In turn, the Michaelis–Menten constant for O_2 (K_o) varied in about the same proportion (ca. threefold) between 183 μM (the Mediterranean angiosperm *Crithmum maritimum* from high osmotic and heat stress environments) and 806 μM (*A. undulatum*). The maximum rate of the carboxylase catalytic turnover (k_{cat}^c) was less variable among the studied species (2.3-fold): *Sideritis cretica* subsp. *spicata* inhabiting

Table 1. Comparative kinetics of Rubisco measured at 25 °C. Parameters shown: the proportion of total leaf-soluble protein that is accounted for by Rubisco ([Rubisco]/[TSP]), the Michaelis–Menten constants for CO_2 (K_c) and O_2 (K_o), the maximum carboxylation rate (k_{cat}^c), and the carboxylation catalytic efficiency (k_{cat}^c/K_c)

Species	[Rubisco]/[TSP] (%)	K_c (μM)	K_o (μM)	k_{cat}^c (s^{-1})	k_{cat}^c/K_c (s^{-1} mM^{-1})
Bryophytes					
Atrichum undulatum	5 ± 1	19.2 ± 0.1	806 ± 100	3.0 ± 0.2	157 ± 9
Marchantia polymorpha	9 ± 1	12.7 ± 0.3	565 ± 64	2.6 ± 0.2	206 ± 14
Ferns					
Pteridium aquilinum	18 ± 1	13.9 ± 0.1	391 ± 14	4.0 ± 0.1	286 ± 4
Platycerium superbum	17 ± 2	12.4 ± 0.2	459 ± 42	2.3 ± 0.1	190 ± 14
Gymnosperms					
Cycas panzhihuaensis	16 ± 1	8.8 ± 0.2	525 ± 21	3.1 ± 0.3	351 ± 36
Metasequoia glyptostroboides	13 ± 1	15.5 ± 1.3	561 ± 68	2.7 ± 0.4	173 ± 22
Basal angiosperm					
Nymphaea alba	15 ± 1	11.2 ± 0.4	438 ± 43	2.4 ± 0.1	215 ± 11
Aquatic macrophyte using HCO_3^-					
Ceratophyllum demersum	5 ± 1	13.6 ± 0.5	317 ± 13	3.5 ± 0.2	256 ± 9
CAM plants					
Agave victoriae–reginae	4 ± 1	9.7 ± 0.4	400 ± 44	3.4 ± 0.1	356 ± 11
Carpobrotus edulis	20 ± 1	9.5 ± 0.2	313 ± 17	3.6 ± 0.1	374 ± 13
Echeveria elegans	8 ± 1	10.5 ± 0.7	236 ± 27	4.5 ± 0.2	435 ± 46
Carnivorous plants					
Drosera capensis	9 ± 2	10.3 ± 0.4	327 ± 24	4.7 ± 0.2	456 ± 29
Drosera venusta	5 ± 1	11.8 ± 0.2	348 ± 5	3.3 ± 0.1	278 ± 8
Sarracenia flava	6 ± 1	12.6 ± 0.1	426 ± 19	4.4 ± 0.1	348 ± 2
C_3 plants from low stress environments					
Arabidopsis thaliana	21 ± 1	9.9 ± 0.4	333 ± 29	4.1 ± 0.3	417 ± 38
Dactylis glomerata cv. Porto	30 ± 1	10.7 ± 0.1	453 ± 79	3.2 ± 0.2	301 ± 17
Eucalyptus moorei	24 ± 1	10.0 ± 0.3	285 ± 11	3.2 ± 0.1	316 ± 12
Eucalyptus neglecta	18 ± 2	7.9 ± 0.2	230 ± 12	2.5 ± 0.1	319 ± 15
Iris douglasiana	21 ± 2	9.7 ± 0.6	413 ± 22	3.5 ± 0.2	364 ± 22
Trachycarpus fortunei	19 ± 1	9.0 ± 0.8	364 ± 21	2.8 ± 0.1	317 ± 23
Triticum aestivum cv. Alexandria	28 ± 1	10.3 ± 0.1	414 ± 7	4.0 ± 0.1	393 ± 8
C_3 plants from environments with high osmotic and heat stress					
Crithmum maritimum	26 ± 2	8.7 ± 0.1	183 ± 31	3.4 ± 0.1	387 ± 11
Limonium latebracteatum	28 ± 1	8.8 ± 1.0	344 ± 7	2.7 ± 0.1	316 ± 33
Limonium stenophyllum	25 ± 1	8.4 ± 0.2	457 ± 36	2.6 ± 0.1	313 ± 17
Limonium virgatum	34 ± 4	8.5 ± 0.2	381 ± 35	2.4 ± 0.1	282 ± 6
Pallenis maritima	29 ± 1	6.4 ± 0.3	321 ± 20	2.7 ± 0.1	433 ± 37
Sideritis cretica subsp. spicata	25 ± 2	7.8 ± 0.1	328 ± 16	2.0 ± 0.3	262 ± 43
Teucrium heterophyllum	23 ± 1	6.7 ± 0.1	359 ± 65	2.7 ± 0.1	401 ± 3

Data are means ± standard errors of three replicates.

environments with high osmotic and heat stress showed the lowest value (2.0 s^{-1}), and the carnivorous plant *Drosera capensis* had the highest value (4.7 s^{-1}). The carboxylase catalytic efficiency (k_{cat}^c/K_c) varied between 157 s^{-1} mM^{-1} (*A. undulatum*) and 456 s^{-1} mM^{-1} (*D. capensis*; Table 1). The proportion of Rubisco relative to total leaf-soluble protein concentration ([Rubisco]/[TSP]) illustrates the relative nitrogen allocation among leaf-soluble proteins. This ratio varied eightfold between 4% (for the CAM species *Agave victoriae-reginae*) and 34% (for *Limonium virgatum* inhabiting environments with high osmotic and heat stress).

There was a clear trend for variation in Rubisco kinetics across the different groups of species (Table 2). Rubisco affinity for CO_2 increased in the following direction: bryophytes < submerged aquatic macrophyte using HCO_3^- < ferns < gymnosperms < carnivorous plants < basal angiosperm < CAM plants < C_3 species from low stress habitats < C_3 species from environments with high osmotic and heat stress (Table 2). The maximum carboxylation rate (k_{cat}^c) increased in the following order: basal angiosperm < C_3 species from environments with high osmotic and heat stress < bryophytes < gymnosperms < ferns < C_3 species from low stress habitats – submerged aquatic macrophyte using HCO_3^- < CAM plants < carnivorous plants (Table 2). The lowest values for k_{cat}^c/K_c were found in bryophytes (below 200 s^{-1} mM^{-1}), followed by ferns, gymnosperms, basal angiosperm and aquatic macrophyte (below 300 s^{-1} mM^{-1}); and the highest values were measured in CAM plants, carnivorous plants, C_3 species from low stress habitats and C_3 species from environments with high osmotic and heat stress (above

Table 2. Comparative Rubisco kinetics of phylogenetic and ecological groups of species: the proportion of total leaf-soluble protein that is accounted for by Rubisco ([Rubisco]/[TSP]), the Michaelis–Menten constants for CO_2 (K_c) and O_2 (K_o), the maximum carboxylation rate (k_{cat}^c), and the carboxylation catalytic efficiency (k_{cat}^c/K_c)

Group	[Rubisco]/[TSP] (%)	K_c (μM)	K_o (μM)	k_{cat}^c (s^{-1})	k_{cat}^c/K_c (s^{-1} mM^{-1})
Bryophytes	7 ± 1^{ab}	16.0 ± 1.5^{e}	685 ± 76^{c}	2.8 ± 0.1^{abc}	181 ± 13^{a}
Ferns	18 ± 1^{d}	13.1 ± 0.3^{cd}	425 ± 25^{a}	3.2 ± 0.4^{bcd}	238 ± 23^{a}
Gymnosperms	14 ± 1^{cd}	12.2 ± 1.6^{cd}	543 ± 33^{b}	2.9 ± 0.2^{abc}	262 ± 44^{a}
Basal angiosperm	15 ± 1^{cd}	11.2 ± 0.4^{bc}	438 ± 43^{ab}	2.4 ± 0.1^{a}	215 ± 11^{a}
Aquatic macrophyte using HCO_3^-	5 ± 1^{a}	13.6 ± 0.5^{d}	317 ± 13^{a}	3.5 ± 0.2^{cde}	256 ± 9^{a}
CAM plants	11 ± 2^{bc}	9.9 ± 0.3^{b}	316 ± 29^{a}	3.8 ± 0.2^{de}	388 ± 19^{b}
Carnivorous plants	7 ± 1^{ab}	11.7 ± 0.4^{bcd}	367 ± 18^{a}	4.1 ± 0.2^{e}	361 ± 27^{b}
C_3 plants from low stress environments	23 ± 1^{e}	9.6 ± 0.2^{ab}	356 ± 20^{a}	3.3 ± 0.1^{bcd}	347 ± 12^{b}
C_3 plants from environments with high osmotic and heat stress	27 ± 1^{e}	7.9 ± 0.3^{a}	339 ± 20^{a}	2.7 ± 0.1^{ab}	342 ± 16^{b}

Data are means ± standard errors. Different letters denote statistically significant differences by Duncan analysis ($P < 0.05$) among groups.

300 s^{-1} mM^{-1}; Table 2). The [Rubisco]/[TSP] ratio was low in bryophytes, carnivorous plants and aquatic macrophyte (below 10%); medium in ferns, gymnosperms, basal angiosperm and CAM plants (below 20%); and high in C_3 angiosperms from low and high stress habitats (above 20%; Table 2).

Intraspecific variability in Rubisco kinetics

Intraspecific variation in Rubisco kinetics was assessed in two crop species, *D. glomerata* and *T. aestivum*. No significant differences were observed in any of the parameters studied between the cultivars of *D. glomerata* (Table 3), which all had identical L-subunit sequences. By contrast, significant variation was observed in k_{cat}^c and K_c, but not in K_o, between the wheat genotypes (Table 3), despite the Rubiscos of the five cultivars having identical *rbc*L sequences.

Correlations among Rubisco kinetic parameters

The [Rubisco]/[TSP] ratio correlated negatively with k_{cat}^c and particularly with K_c when all groups were considered [Table 4, Pearson's (linear) correlation coefficients, PCC]. Thus, those species having a higher proportion of leaf-soluble protein in the form of Rubisco, also showed higher affinity for CO_2 (lower K_c) and lower velocity of carboxylation per catalytic site (lower k_{cat}^c; Fig. 1a). Remarkably, the correlation between K_c and k_{cat}^c was not significant when all groups were included (Table 4, PCC), although it was significant within the group of modern angiosperms, Mesangiospermae (Fig. 1b). Bryophytes, ferns, gymnosperms and basal and aquatic angiosperms behaved as outliers within the relationship between K_c and k_{cat}^c, leading to variable values for k_{cat}^c/K_c (Table 2). The two affinity constants (K_c and K_o) showed a significant positive correlation (Table 4, PCC) with the implication that evolution towards increased Rubisco affinity for CO_2 is inevitably accompanied by simultaneous increases in the affinity for O_2 (Fig. 1c). Finally, a negative relationship was observed between K_o and k_{cat}^c/K_c (Table 4, PCC), indicating that increases in the Rubisco affinity for O_2 were paralleled by decreases in the carboxylase catalytic efficiency.

Some of the correlations between Rubisco kinetic parameters changed when corrected for the phylogenetic signal. The PIC correlations of [Rubisco]/[TSP] versus k_{cat}^c, K_c

Table 3. Intraspecific variation in Rubisco kinetics in *Triticum aestivum* and *Dactylis glomerata* measured at 25 °C

Species	[Rubisco]/[TSP] (%)	K_c (μM)	K_o (μM)	k_{cat}^c (s^{-1})	k_{cat}^c/K_c (s^{-1} mM^{-1})
Triticum aestivum cv. Alexandria	28 ± 1^{b}	10.3 ± 0.1^{b}	414 ± 7	4.0 ± 0.1^{bc}	393 ± 8^{a}
Triticum aestivum genotype 1	21 ± 1^{a}	10.5 ± 0.2^{b}	407 ± 21	4.3 ± 0.1^{c}	404 ± 5^{ab}
Triticum aestivum genotype 2	31 ± 2^{b}	9.3 ± 0.2^{a}	376 ± 8	4.0 ± 0.1^{bc}	436 ± 8^{c}
Triticum aestivum genotype 3	30 ± 1^{b}	9.1 ± 0.1^{a}	345 ± 24	3.7 ± 0.1^{a}	412 ± 5^{ab}
Triticum aestivum genotype 4	35 ± 1^{c}	9.6 ± 0.2^{a}	408 ± 33	4.0 ± 0.1^{b}	416 ± 8^{bc}
Dactylis glomerata cv. Jana	24 ± 1^{a}	9.8 ± 0.4	419 ± 33	3.4 ± 0.2	345 ± 12
Dactylis glomerata cv. Kasbah	28 ± 1^{b}	11.2 ± 1.6	524 ± 131	3.0 ± 0.3	273 ± 39
Dactylis glomerata cv. Porto	30 ± 1^{b}	10.7 ± 0.1	453 ± 79	3.2 ± 0.2	301 ± 17

Wheat genotypes 1–4 originated in Mexico and were selected on the basis of their resistance to drought stress. The proportion of total leaf-soluble protein that is accounted for by Rubisco ([Rubisco]/[TSP]), the Michaelis–Menten constants for CO_2 (K_c) and O_2 (K_o), the maximum carboxylation rate (k_{cat}^c) and the carboxylation catalytic efficiency (k_{cat}^c/K_c). Data are means ± standard errors of three replicates. Different letters denote statistically significant differences by Duncan analysis ($P < 0.05$) among genotypes or varieties within the same species.

Table 4. Phylogenetically independent contrast (PIC) correlation coefficients (upper right of the diagonal) and Pearson's correlation coefficients (PCC, lower left of the diagonal) between Rubisco content and kinetic parameters of 28 plant species

	[Rubisco]/[TSP]	K_c	k_{cat}	k_{cat}/K_c	K_o
[Rubisco]/[TSP]		–0.517***	–0.273	0.193	–0.107
K_c	–0.601***		0.314	–0.556***	0.193
k_{cat}	–0.352*	0.175		0.614***	–0.090
k_{cat}/K_c	0.268	–0.708***	0.552***		–0.241
K_o	–0.231	0.587***	–0.223	–0.631***	

The concentration of total leaf-soluble protein being Rubisco ([Rubisco]/[TSP]), the Michaelis–Menten constants for CO_2 (K_c) and O_2 (K_o), the maximum carboxylation rate (k_{cat}^c) and the carboxylation catalytic efficiency (k_{cat}^c/K_c). Data were log-transformed before independent contrasts and Pearson's correlation. Traits that are significantly correlated are marked: ***$P < 0.005$; **$P < 0.01$; *$P < 0.05$.

versus K_o and K_o versus k_{cat}^c/K_c were not significant, but the relationship [Rubisco]/[TSP] versus K_c maintained significant correlation after consideration of the phylogenetic relations between species (Table 4). PIC correlations tend to increase after including data for all 34 plant species and cultivars, as compared with the above analyses for the 28 different species (compare Table 4 and Supporting Information Table S1). The correlations [Rubisco]/[TSP] versus k_{cat}^c and k_{cat}^c versus K_c became significant ($P < 0.05$) when more data points were included. The analyses with and without the incorporation of evolutionary relationships as well as including wheat and *D. glomerata* as multiple or single entries were mostly consistent, indicating that the detected patterns reflected coordinated evolution. A significant PIC correlation between traits (Table 4) indicates that they have changed in a similar direction and extent across the phylogeny and supports the hypothesis that there is a functional link between these traits.

L-subunit residues under positive selection, which are potentially associated with Rubisco kinetics

Bayes Empirical Bayes algorithm implemented in PAML (Yang *et al*. 2005) identified L-subunit residues under positive selection along phylogenetic branches leading to species with high and low K_c, high k_{cat}^c and low K_o, but not along branches leading to species with low k_{cat}^c and high K_o (Table 5). The total number of sites under positive selection was thirteen, L-subunit residues 86, 95, 99, 116, 142, 228, 258, 281, 282, 320, 328, 367 and 439. Selected residues were located at different positions within the Rubisco tertiary structure and included functionally diverse sites participating in L-subunit intradimer and dimer–dimer interactions, interactions with small subunits (S-subunits) and with Rubisco activase (Table 5).

DISCUSSION

The Rubisco kinetic variation reported in the present study shows a trend towards increasing affinity for CO_2 and carboxylation catalytic efficiency (k_{cat}^c/K_c), on proceeding from more basal groups of land plants, which originated during periods of relatively high atmospheric [CO_2], to more recent groups that emerged during subsequent periods of lower atmospheric [CO_2]. Thus, the lowest affinity for CO_2 (i.e. highest K_c) and k_{cat}^c/K_c were found in bryophytes, which are the oldest phylogenetic group of land plants, which originated over 470 million years ago, when the atmospheric [CO_2] exceeded several thousand ppm and the [CO_2]/[O_2] ratio was at its highest – approximately 0.02 (Kenrick & Crane 1997; Haworth *et al*. 2011; Ligrone *et al*. 2012). The polypod ferns, *Pteridium aquilinum* and *Platycerium superbum*, belonging to one of the basal lineages among the vascular plants, which diversified during the Early Cretaceous under high [CO_2] and elevated [CO_2]/[O_2] ratios (Schuettpelz & Prier 2009), also showed high values of K_c. Among the vascular plants, the highest K_c value was found in the gymnosperm *Metasequoia glyptostroboides* (Coniferales, i.e. conifers; Table 1), a living-fossil species, which originated early in the Late Cretaceous (Liu *et al*. 1999; Mao *et al*. 2012), when the atmospheric [CO_2] was also above 1000 ppm and the [CO_2]/[O_2] approximately 0.01 (Haworth *et al*. 2011). By contrast, Rubisco of the gymnosperm *Cycas panzhihuaensis* (Cycadales, i.e. cycads) showed ca. twofold higher affinity for CO_2 than that of *M. glyptostroboides*. Low and high K_c for Rubisco has already been reported in cycads and conifers, respectively (Yeoh *et al*. 1981). This difference between the two gymnosperms can be explained as follows. Firstly, cycads are considered to be the most primitive extant seed-bearing plants whose origins have been traced to the Lower Permian when the [CO_2]/[O_2] ratio had the closest value to current day levels (Mamay 1969; Soltis *et al*. 2002; Salas-Leiva *et al*. 2013), whereas conifers mostly diversified in the Jurassic to Cretaceous (*M. glyptostroboides* in Early to Late Cretaceous, Mao *et al*. 2012), with much higher [CO_2] (Berner 2006). Secondly, *M. glyptostroboides* is a fast-growing deciduous tree possessing leaves with relatively low specific leaf area. Contrary to *Metasequoia*, *Cycas* is a slow-growing plant that has evergreen leaves with high specific leaf area (Willis & McElwain 2002), which may increase the leaf diffusive resistance to the passage of CO_2 to the chloroplast stroma (J. Gago *et al*. unpublished). Actually, leaf gas exchange measurements revealed low photosynthetic CO_2 assimilation rates in *Cycas* (Marler 2004).

Angiosperm species showed higher affinity for CO_2 (i.e., lower K_c) and carboxylation catalytic efficiency (k_{cat}^c/K_c) compared with the earlier groups (Table 2). Interestingly, *Nymphaea alba*, a basal angiosperm dating from the earliest

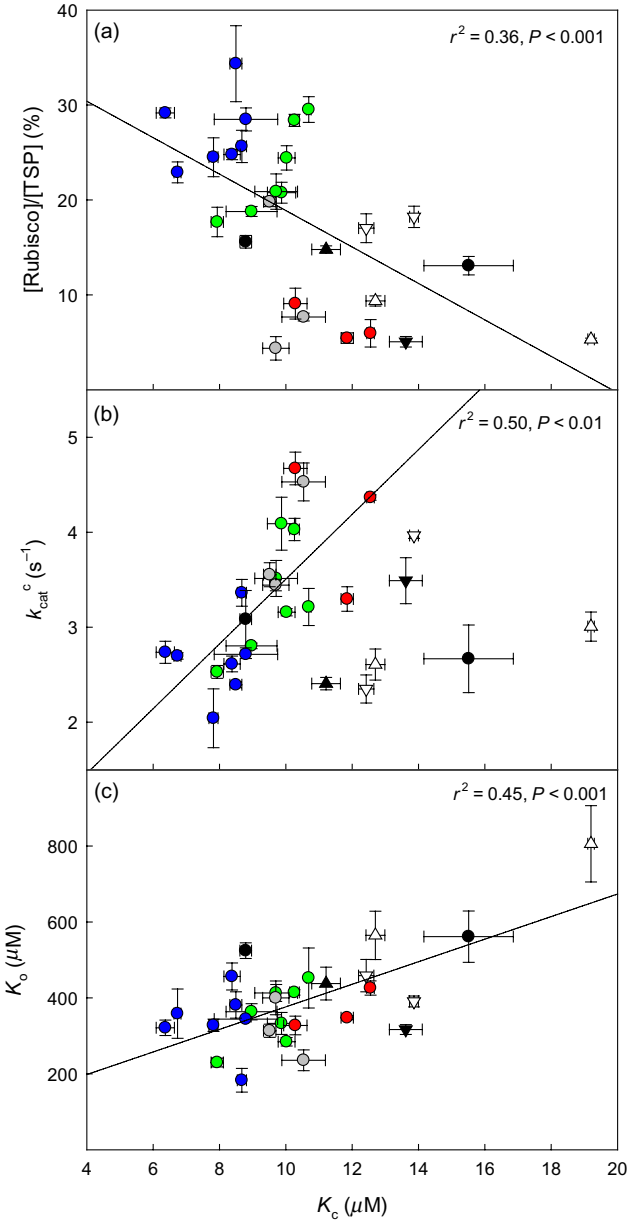

Figure 1. The relationship between the Michaelis–Menten constant for CO_2 (K_c) and (a) the percentage of total leaf-soluble protein being Rubisco, (b) the turnover rate for the carboxylase reaction (k_{cat}^c) and (c) the Michaelis–Menten constant for O_2 (K_o). Species groups and symbols as follows: bryophytes (△), ferns (▽), gymnosperms (●), basal angiosperm (▲), submerged aquatic macrophyte using HCO_3^- (▼), species with the crassulacean acid metabolism (◌), carnivorous plants (●), C_3 plants from low stress environments (●) and C_3 plants from environments with high osmotic and heat stress (●). The regression coefficients were calculated considering all data in plot, except in (b), where bryophytes, ferns, gymnosperms, basal angiosperm and submerged aquatic macrophyte using HCO_3^- were not considered.

Cretaceous (Friis *et al.* 2001; Feild & Arens 2007; Moore *et al.* 2007, 2010), during which the $[CO_2]/[O_2]$ ratio was at its highest since the advent of the angiosperms (Haworth *et al.* 2011), had relatively high K_c and the lowest k_{cat}^c/K_c among angiosperms, compared with the groups that originated in times of lower atmospheric $[CO_2]$. Measurements of Rubisco kinetics in other basal angiosperms from the orders Amborellales, Nymphaeales and Austrobaileyales, all of which originated in time of higher $[CO_2]$ compared with the rest of angiosperms (Mesangiospermae) would be required to test whether our findings of high K_c and low k_{cat}^c/K_c in the basal angiosperm *Nymphaea alba* is a part of general trend. Overall, the present comparison of the basal and more recent lineages of land plants supports the co-evolution of Rubisco affinity for CO_2 and carboxylation catalytic efficiency (k_{cat}^c/K_c), in response to changes in atmospheric $[CO_2]$ during the evolution of land plants.

This evolutionary trend towards decreased K_c was mirrored by equivalent decreases in K_o (Fig. 1c). Constant K_c/K_o ratio would be in agreement with the hypothesis that the maintenance of a certain oxygenation capacity was important during the diversification of terrestrial plants as an energy sink under high light environments (André 2011). A consequence of constant K_c/K_o is that the increase in the $S_{c/o} = [(k_{cat}^c K_o)/(k_{cat}^o K_c)]$ has been achieved mostly through alterations of the ratio between the maximum velocities for carboxylation and oxygenation (k_{cat}^c/k_{cat}^o). It has been argued that interdependence of kinetic parameters is regulated structurally (Tcherkez 2013). Our analysis indicates that selection for low K_o was important, with five amino acid substitutions under positive selection (Table 5). Of these, only the residue at position 86 was also under positive selection along branches leading to species with low K_c.

The observed trends for Rubisco kinetics in C_3 species inhabiting environments with high osmotic and heat stress are in agreement with previous results (Galmés *et al.* 2005), demonstrating that Rubisco has evolved towards higher affinity for CO_2 at the expenses of decreasing k_{cat}^c (Fig. 1b; Table 2). Low CO_2 availability (provoked by low water availability) and high temperature, both favour photorespiration, forcing Rubisco to optimize towards decreased K_c. Hence, C_3 species inhabiting highly stressful environments presented the lowest k_{cat}^c (Table 2). Conversely, carnivorous plants presented on average the highest k_{cat}^c, which may also be related to photosynthetic optimization under extremely low Rubisco content (see below).

The trade-off between Rubisco affinity for CO_2 and its catalytic rate has been reported and discussed before (e.g. Tcherkez *et al.* 2006; Kubien *et al.* 2008; Savir *et al.* 2010); and our data confirm the positive correlation between K_c and k_{cat}^c although correlation coefficients substantially vary depending on which taxa are included (Fig. 1b; Table 4 and Supporting Information S1). The same applies to other studies investigating K_c and k_{cat}^c relations, for example, Savir *et al.* (2010) used the dataset that included 28 Rubiscos from 27 organisms representing bacteria, algae and C_3 and C_4 flowering plants (but no bryophytes, ferns and gymnosperms) and found a strong correlation between K_c and k_{cat}^c. In order to make a direct comparison with our findings, we applied PIC to reanalyse the whole dataset of Savir *et al.* (2010) as well as its subsets containing only flowering plants and all other taxa, respectively. Correlation coefficient (r) is higher in Savir *et al.*

Table 5. Amino acid (AA) substitutions shown to be under positive selection by the Bayes empirical Bayes (BEB) analysis (Yang *et al.* 2005) along branches leading to species with certain Rubisco properties

Residue[a]	AA changes			Location of residue	Structural motifs within 5 Å	Interactions[b]
Branches leading to species with $K_c \leq 9.0$						
86*	H, D	→	E, G	Strand C	Strands A, C, D	*RA*
95*	N, T	→	D, S		Strands B, D, E	ID, *RA*
Branches leading to species with $K_c \geq 11.0$						
116**	M	→	L			ID
282*	H	→	F	Helix 4	Helixes 4, 5	DD, SSU
Branches leading to species with $k_{cat}^c \geq 4.0$						
228*	A	→	S	Helix 2	Helixes 1, 2	SSU
258***	R	→	Y	Helix 3	Helix 3	DD, SSU
Branches leading to species with $K_o \leq 400.0$						
86***	D, H	→	E, G	Strand C	Strands A, C, D	*RA*
99*	A	→	C, V	Strand D	Strands B, C, D	
142***	P	→	I, T, V	Helix D	N-terminus; strands D, H	DD
281**	A	→	S	Helix 4	Helixes 4, 5	DD, SSU
320**	M	→	L	Helix 5	Helix 5	DD
328***	A	→	S	Loop 6	AS; loop 6 region; helixes 5, 7; strand 7	AS
367**	D	→	P, S	Strand H	Strand H; helix 6	DD
439***	R	→	A, S, T, V	Helix G	Helix G	

[a]Residue numbering is based on the spinach sequence. Bayesian posterior probability values: *>0.90, **>0.95, ***>0.99.
[b]Interactions in which the selected residues and/or residues within 5 Å of them are involved. AS, interactions with the active site; ID, intradimer interactions; DD, dimer–dimer interactions; RA, interface for interactions with Rubisco activase; SSU, interactions with small subunits; interactions based on literature survey only are given in italics; after (Spreitzer and Salvucci, 2002; Ott *et al.*, 2000; Du *et al.*, 2003).

(2010) study: PIC *r* was 0.73, when all taxa were included. However, when K_c and k_{cat}^c of bacterial and algal Rubisco were analysed separately, PIC *r* increased to 0.78. By contrast, when only the data from flowering plants of Savir *et al.* (2010) were included in the analysis, the corresponding value of *r* dropped to 0.49, indicating the importance of bacterial and algal Rubisco to the high correlation coefficients reported there. Although our dataset is less diverse phylogenetically than that of Savir *et al.* (2010), it includes groups that were not represented there, as well as more comprehensive phylogenetic coverage of land plants in general, and flowering plants in particular. Our dataset shows variable strength of correlation between K_c and k_{cat}^c among angiosperms and other land plants. PIC correlation coefficient *r* for the whole dataset was 0.31, which increased to 0.43 for angiosperms only, and to 0.52 for angiosperms only omitting the basal angiosperm, *Nymphaea alba*, and the submerged aquatic macrophyte utilizing HCO_3^-, *Ceratophyllum demersum*. Thus, the numbers become similar to the angiosperm subset from Savir *et al.* (2010). In contrast, 'outliers' consisting of bryophytes, ferns, gymnosperms and the two angiosperms mentioned above (Fig. 1b), when analysed as a separate group had a PIC correlation coefficient of 0.21 only. These findings show that although positive correlation between K_c and k_{cat}^c exists across the whole Rubisco spectrum and its subsets, the correlation strength varies significantly among different phylogenetic groups that differ in ecology and physiology as well as Rubisco structure. It is worth mentioning that k_{cat}^c could be underestimated during *in vitro* kinetics assays. If k_{cat}^c underestimation occurred predominantly in some of the species located to the right in Fig. 1b, that would mean that their k_{cat}^c/K_c ratio is higher than assayed and thus closer to the boundary relationship found for the majority of species.

The pioneering comparison of K_c among C_3, C_4, CAM and aquatic C_3 species using carbon concentration mechanisms (CCM) by Yeoh *et al.* (1981) showed that CAM had similar affinities but that Rubisco from aquatic species had lower affinity for CO_2 compared with C_3 Rubisco. The data in this study confirms and extends these observations. There were no significant differences between CAM and C_3 species from non-stressful environments, in any of the kinetic traits studied (Table 2). However, Rubisco of CAM plants inhabiting arid environments characterized by water deficit showed higher values for K_c and k_{cat}^c than those of C_3 species from similar environments (Table 2). Although both groups are affected by water stress, in CAM plants Rubisco is exposed daily to a range of CO_2 concentrations (100 to 2000 ppm) equivalent to those occurring throughout much of Earth's history and much higher compared with C_3 plants (Griffiths 2006). It is possible that these conditions hinder a clear relationship between such Rubisco traits and the operating CO_2 concentration in CAM plants. In contrast to CAM plants, *Ceratophyllum demersum*, a submerged aquatic macrophyte utilizing HCO_3^-, showed the opposite trends. *C. demersum* had the highest K_c and one of the lowest carboxylation catalytic efficiency (k_{cat}^c/K_c) values among the angiosperms analysed (Table 2), resembling Rubisco from C_4 plants – an angiosperm group possessing highly efficient CCM (Yeoh *et al.* 1981; Kubien *et al.* 2008).

The [Rubisco]/[TSP] ratio was found to be more variable than any of the kinetic parameters included in the study, and this variability could be explained by phylogenetic and environmental constraints (Table 2). Conventional statistics

revealed inverse relationships between [Rubisco]/[TSP] and K_c and k_{cat}^c (Table 4). These correlations may suggest that species, which evolved faster or lower affinity versions of the enzyme, could succeed with a lower [Rubisco]/[TSP]. These trends may be a result of Rubisco optimization under different photosynthetic limitations. Low [Rubisco]/[TSP] could be indicative of Rubisco-limited photosynthesis, under which k_{cat}^c has a dominant role in determining the maximum (presumably Rubisco limited) CO_2 assimilation rate (Farquhar *et al*. 1980). By contrast, if high [Rubisco]/[TSP] is related to predominantly RuBP-limited photosynthesis, then k_{cat}^c is no longer decisive in governing the maximum CO_2 assimilation rate. Instead, the biochemical model of leaf photosynthesis shows that, under RuBP-limited conditions, the specificity factor becomes the sole Rubisco kinetic parameter directly determining the maximum CO_2 assimilation rate (Farquhar *et al*. 1980). Rubisco specificity factor is positively related with the enzyme affinity for CO_2 (i.e. $1/K_c$) and negatively with k_{cat}^c (Tcherkez *et al*. 2006; Savir *et al*. 2010). Irrespective of these trends, the lowest [Rubisco]/[TSP] ratio was found among plants living in habitats with low nitrogen (bryophytes, aquatic macrophytes, carnivorous and CAM plants), which interestingly incorporated the worst and the best examples of Rubisco performance in terms of k_{cat}^c/K_c (Table 2).

Significant differences were detected in k_{cat}^c and K_c among different genotypes of *Triticum aestivum* (Table 3). Although the range of variation was modest and such differences were not apparent in *Dactlytis glomerata*, these results are relevant because they indicate that variability in Rubisco kinetics is feasible among genotypes or cultivars of the same crop species. Significant intraspecific variability in Rubisco kinetic parameters was previously reported in another grass crop, *Hordeum vulgare* (Rinehart *et al*. 1983). In the case of identical L-subunits, it is logical to assume that any kinetic differences are caused by sequence diversity among the S-subunits, and/or by different combinations of distinct S-subunits within the Rubisco holoenzyme (which contains 8 L- and 8 S-subunits). Hexaploid wheat, *T. aestivum*, possesses at least 22 S-subunit genes (*rbc*S) encoding different S-subunits (Galili *et al*. 1998). By comparison, *Arabidopsis thaliana* has only four *rbc*S genes. This unusually high number could underpin distinct Rubisco holoenzymes, differentiated according to S-subunit composition. Although Rubisco active sites are located in the L-subunits, Ishikawa *et al*. (2011) showed significant changes in Rubisco kinetics when rice S-subunit was replaced with sorghum S-subunit, providing evidence for a differential role of S-subunits in Rubisco kinetics. This approach may be enhanced by the discovery of significant variability in the kinetic constants – together with the associated molecular mechanisms – among genotypes of economically important crops.

Ten Rubisco L-subunit residues under positive selection, which have been reported in this study (residues 86, 95, 142, 228, 258, 281, 282, 320, 328, 439), had been reported previously (Kapralov & Filatov 2007; Christin *et al*. 2008; Iida *et al*. 2009; Kapralov *et al*. 2012), while three had not (residues 99, 116, 367). This implies that Rubisco has a relatively limited number of residue positions responsible for kinetic 'fine-tuning'. This study is the first in which sequence analysis has been conducted in parallel with kinetic measurements, allowing identification of amino acid substitutions likely to be associated with specific changes in Rubisco kinetics as well as providing further information, insights and impetus to Rubisco engineering as a tool for crop improvement.

Concluding remarks

Unquestionably, CO_2 fixation by Rubisco represents the predominant rate-limiting step in the photosynthetic process. Two major strategies have evolved and serve as functional solutions to this limitation: CO_2-concentrating mechanisms to supply Rubisco with high levels of CO_2, and optimization of Rubisco kinetic constants to the prevailing environmental conditions (Bainbridge *et al*. 1995; Raven 2000). Previous assessments of evolutionary trends of Rubisco kinetics have been mostly based on the compilation of data from different laboratories using diverse techniques (e.g. Badger & Andrews 1987; Kent & Tomany 1995; Badger *et al*. 1998; Tcherkez *et al*. 2006; Savir *et al*. 2010; Whitney *et al*. 2011a). The present study is one of the largest inputs of new data on various Rubisco kinetic parameters, measured using identical techniques for all species tested, and thus minimizing differences due to factors not directly related to the properties of the enzyme.

The present dataset provides new insights on the diversity of the kinetic properties of Rubisco across different groups of land plants. The results confirm that evolution of Rubisco in land plants is likely to have been complementary to the simultaneously changing atmospheric $[CO_2]$ and $[O_2]$, as well as to adaptations in leaf architecture, morphology and conductance (Beerling *et al*. 2001; Franks & Beerling 2009; Haworth *et al*. 2011). In particular, the data indicate that falling $[CO_2]/[O_2]$ ratios are linked to Rubisco innovation towards increased affinity for CO_2. During the evolution of land plants, we observed a trend for an increased Rubisco affinity for CO_2 and increased carboxylase catalytic efficiency (k_{cat}^c/K_c), concomitant with increases in the proportion of leaf-soluble protein accounted for by Rubisco. In addition, the high variability in the ratio k_{cat}^c/K_c among groups indicates that deviations from the apparent trade-off between Rubisco velocity and affinity exist in nature. Hence, Rubisco kinetic properties from highly specialized groups – carnivorous and CAM species, along with C_3 species from water-stress habitats – presented improved performance by means of higher k_{cat}^c/K_c. Overall, the present study suggests that exploration of the natural variability of Rubisco kinetic properties, particularly among species subject to extreme environments, in combination with analyses of the corresponding Rubisco-encoding genes, is a potent means of identifying candidate amino acid replacements to underpin a knowledge-based, molecular approach to the optimization of crop photosynthesis under a range of environmental conditions.

ACKNOWLEDGMENTS

This research was supported by projects AGL2009-07999 and BFU2011-23294 (Plan Nacional, Spain) awarded to J.G. and J.F., respectively. P.J.A. and M.A.J.P. are supported by the BBSRC 20:20 Wheat® Institute Strategic Program (BBSRC BB/J/00426X/1) and BBSRC BB/I002545/1 and BB/I017372/1. Maria T. Moreno is acknowledged for assistance during measurements of Rubisco kinetics. The authors declare no conflict of interest.

REFERENCES

Andersson I. & Backlund A. (2008) Structure and function of Rubisco. *Plant Physiology and Biochemistry* **46,** 275–291.

André M.J. (2011) Modelling $^{18}O_2$ and $^{16}O_2$ unidirectional fluxes in plants: II. Analysis of Rubisco evolution. *Bio Systems* **103,** 252–264.

Badger M.R. & Andrews T.J. (1987) Co-evolution of Rubisco and CO_2 concentrating mechanisms. In *Progress in Photosynthesis Research* (ed J. Biggins) Vol. III, pp. 601–609. Martinus Nijhoff Publishers, Dordrecht, the Netherlands.

Badger M.R., Andrews T.J., Whitney S.M., Ludwig M., Yellowlees D.C., Leggat W. & Price G.D. (1998) The diversity and coevolution of Rubisco, plastids, pyrenoids, and chloroplast-based CO_2- concentrating mechanisms in algae. *Canadian Journal of Botany* **76,** 1051–1071.

Bainbridge G., Madgwick P., Parmar S., Mitchell R., Paul M., Pitts J., . . . Parry M.A.J. (1995) Engineering Rubisco to change its catalytic properties. *Journal of Experimental Botany* **46,** 1269–1276.

Beerling D.J., Osborne C.P. & Chaloner W.G. (2001) Evolution of leaf-form in land plants linked to atmospheric CO_2 decline in the Late Palaeozoic era. *Nature* **410,** 352–354.

Berner R.A. (2006) GEOCARBSULF: a combined model for Phanerozoic atmospheric O_2 and CO_2. *Geochimica et Cosmochimica Acta* **70,** 5653–5664.

Bird I.F., Cornelius M.J. & Keys A.J. (1982) Affinity of RuBP carboxylases for carbon dioxide and inhibition of the enzymes by oxygen. *Journal of Experimental Botany* **33,** 1004–1013.

Carmo-Silva A.E., Keys A.J., Andralojc P.J., Powers S.J., Arrabaça M.C. & Parry M.A.J. (2010) Rubisco activities, properties, and regulation in three different C4 grasses under drought. *Journal of Experimental Botany* **61,** 2355–2366.

Christin P.-A., Salamin N., Muasya A.M., Roalson E.H., Russier F. & Besnard G. (2008) Evolutionary switch and genetic convergence on *rbc*L following the evolution of C4 photosynthesis. *Molecular Biology and Evolution* **25,** 2361–2368.

Cuénoud P., Savolainen V., Chatrou L.W., Powell M., Grayer R.J. & Chase M.W. (2002) Molecular phylogenetics of Caryophyllales based on nuclear 18S rDNA and plastid *rbc*L, atpB, and matK DNA sequences. *American Journal of Botany* **89,** 132–144.

Delgado E., Medrano H., Keys A.J. & Parry M.A. (1995) Species variation in Rubisco specificity factor. *Journal of Experimental Botany* **46,** 1775–1777.

Du Y.C., Peddi S.R. & Spreitzer R.J. (2013) Assessment of structural and functional divergence far from the large subunit active site of Ribulose-1,5-bisphosphate carboxylase/oxygenase. *Journal of Biological Chemistry* **278,** 49401–49405.

Farquhar G., von Caemmerer S. & Berry J. (1980) A biochemical-model of photosynthetic CO_2 assimilation in leaves of C_3 species. *Planta* **149,** 78–90.

Feild T.S. & Arens N.C. (2007) The ecophysiology of early angiosperms. *Plant, Cell & Environment* **30,** 291–309.

Felsenstein J. (1985) Phylogenies and the comparative method. *The American Naturalist* **125,** 1–15.

Franks P.J. & Beerling D.J. (2009) Maximum leaf conductance driven by CO_2 effects on stomatal size and density over geologic time. *Proceedings of the National Academy of Sciences of the United States of America* **106,** 10343–10347.

Friis E.M., Pedersen K.R. & Crane P.R. (2001) Fossil evidence of water lilies (Nymphaeales) in the Early Cretaceous. *Nature* **410,** 357–360.

Galili S., Avivi Y. & Feldman M. (1998) Differential expression of three RbcS subfamilies in wheat. *Plant Science* **139,** 185–193.

Galmés J., Flexas J., Keys A.J., Cifre J., Mitchell R.A.C., Madgwick P.J., . . . Parry M.A.J. (2005) Rubisco specificity factor tends to be larger in plant species from drier habitats and in species with persistent leaves. *Plant, Cell and Environment* **28,** 571–579.

Galmés J., Ribas-Carbó M., Medrano H. & Flexas J. (2011) Rubisco activity in Mediterranean species is regulated by the chloroplastic CO_2 concentration under water stress. *Journal of Experimental Botany* **62,** 653–665.

Galmés J., Conesa M.À., Díaz-Espejo A., Mir A., Perdomo J.A., Niinemets Ü. & Flexas J. (2014) Rubisco catalytic properties optimized for presentand future climatic conditions. *Plant Science* http://dx.doi.org/10.1016/j.plantsci.2014.01.008.

Ghannoum O., Evans J.R., Chow W.S., Andrews T.J., Conroy J.P. von & Caemmerer S. (2005) Faster Rubisco is the key to superior nitrogen-use efficiency in NADP-malic enzyme relative to NAD-malic enzyme C_4 grasses. *Plant Physiology* **137,** 638–650.

Griffiths H. (2006) Plant biology: designs on Rubisco. *Nature* **441,** 940–941.

Haworth M., Kingston C. & McElwain J.C. (2011) Stomatal control as a driver of plant evolution. *Journal of Experimental Botany* **62,** 2419–2423.

Iida S., Miyagi A., Aoki S., Ito M., Kadono Y. & Kosuge K. (2009) Molecular adaptation of *rbcL* in the heterophyllous aquatic plant *Potamogeton*. *PLoS ONE* **4,** e4633.

Ishikawa C., Hatanaka T., Misoo S. & Fukayama H. (2009) Screening of high k_{cat} Rubisco among Poaceae for improvement of photosynthetic CO_2 assimilation in rice. *Plant Production Science* **12,** 345–350.

Ishikawa C., Hatanaka T., Misoo S., Miyake C. & Fukayama H. (2011) Functional incorporation of sorghum small subunit increases the catalytic turnover rate of rubisco in transgenic rice. *Plant Physiology* **156,** 1603–1611.

Jordan D.B. & Ogren W.L. (1981) Species variation in the specificity of ribulose-bisphosphate carboxylase-oxygenase. *Nature* **291,** 513–515.

Kaplan W. & Littlejohn T.G. (2001) Swiss-PDB Viewer (Deep View). *Briefings in Bioinformatics* **2,** 195–197.

Kapralov M.V. & Filatov D.A. (2007) Widespread positive selection in the photosynthetic Rubisco enzyme. *BMC Evolutionary Biology* **7,** 73.

Kapralov M.V., Kubien D.S., Andersson I. & Filatov D.A. (2011) Changes in Rubisco kinetics during the evolution of C_4 photosynthesis in *Flaveria* (Asteraceae) are associated with positive selection on genes encoding the enzyme. *Molecular Biology and Evolution* **28,** 1491–1503.

Kapralov M.V., Smith J.A.C. & Filatov D.A. (2012) Rubisco evolution in C_4 eudicots: an analysis of Amaranthaceae *sensu lato*. *PLoS ONE* **7,** e52974.

Karkehabadi S., Taylor T.C. & Andersson I. (2003) Calcium supports loop closure but not catalysis in Rubisco. *Journal of Molecular Biology* **344,** 65–73.

Kenrick P. & Crane P.R. (1997) The origin and early evolution of plants on land. *Nature* **389,** 33–39.

Kent S.S. & Tomany M.J. (1995) The differential of the ribulose 1,5-bisphosphate carboxylase/oxygenase specificity factor among higher plants and the potential for biomass enhancement. *Plant Physiology and Biochemistry* **33,** 71–80.

Keys A.J. (1986) Rubisco: its role in photorespiration. *Philosophical Transactions of the Royal Society B: Biological Sciences* **313,** 325–336.

Kubien D.S., Whitney S.M., Moore P.V. & Jesson L.K. (2008) The biochemistry of Rubisco in *Flaveria*. *Journal of Experimental Botany* **59,** 767–1777.

Ligrone R., Duckett J.G. & Renzaglia K.S. (2012) Major transitions in the evolution of early plants: a bryological perspective. *Annals of Botany* **109,** 851–872.

Liu Y.-J., Li C.-S. & Wang Y.-F. (1999) Studies on fossil Metasequoia from NE China and their taxonomic implications. *Botanical Journal of the Linnean Society* **130,** 267–297.

Ott C.M., Smith B.D., Portis A.R. Jr. & Spreitzer R.J. (2000) Activase region on chloroplast Ribulose-1,5-bisphosphate carboxylase/oxygenase. *Journal of Biological Chemistry* **275,** 26241–26244.

Mamay S.H. (1969) Cycads: fossil evidence of Late Paleozoic origin. *Science* **164,** 295–296.

Mao K., Milne R.I., Zhang L., Peng Y., Liu J., Thomas P., . . . Renner S.S. (2012) Distribution of living Cupressaceae reflects the breakup of Pangea. *Proceedings of the National Academy of Sciences of the United States of America* **109,** 7793–7798.

Marler T.E. (2004) Leaf physiology of shade-grown *Cycas micronesica* leaves following removal of shade. *The Botanical Review* **70,** 63–71.

Masuzaki H., Shimamura M., Furuki T., Tsubota H., Yamaguchi T., Majid H.M.A. & Deguchi H. (2010) Systematic position of the enigmatic liverwort Mizutania (Mizutaniaceae, Marchantiophyta) inferred from molecular phylogenetic analyses. *Taxon* **59,** 448–458.

Moore M.J., Bell C.D., Soltis P.S. & Soltis D.E. (2007) Using plastid genome-scale data to resolve enigmatic relationships among basal angiosperms. *Proceedings of the National Academy of Sciences of the United States of America* **104,** 19369–19374.

Moore M.J., Soltis P.S., Bell C.D., Burleigh J.G. & Soltis D.E. (2010) Phylogenetic analysis of 83 plastid genes further resolves the early diversification of eudicots. *Proceedings of the National Academy of Sciences of the United States of America* **107,** 4623–4628.

Niinemets Ü., Wright I.J. & Evans J.R. (2009) Leaf mesophyll diffusion conductance in 35 Australian sclerophylls covering a broad range of foliage structural and physiological variation. *Journal of Experimental Botany* **60,** 2433–2449.

Nisbet E.G., Grassineau N.V., Howe C.J., Abell P.I., Regelous M. & Nisbet R.E.R. (2007) The age of RubisCO: the evolution of oxygenic photosynthesis. *Geobiology* **5,** 311–355.

Parry M., Madgwick P., Carvalho J. & Andralojc P. (2007) Prospects for increasing photosynthesis by overcoming the limitations of Rubisco. *Journal of Agricultural Science* **145,** 31–43.

Raven J.A. (2000) Land plant biochemistry. *Philosophical Transactions of the Royal Society B: Biological Sciences* **355,** 833–846.

Reynolds M., Foulkes M.J., Slafer G.A., Berry P., Parry M.A.J., Snape J.W. & Angus W.J. (2009) Rising yield potential in wheat. *Journal of Experimental Botany* **60,** 1899–1918.

Rinehart C.A., Tingey S.V. & Andersen W.R. (1983) Variability of reaction kinetics for Ribulose-1,5-bisphosphate carboxylase in a barley population. *Plant Physiology* **72,** 76–79.

Salas-Leiva D.E., Meerow A.W., Calonje M., Griffith M.P., Francisco-Ortega J., Nakamura K., . . . Namoff S. (2013) Phylogeny of the cycads based on multiple single-copy nuclear genes: congruence of concatenated parsimony, likelihood and species tree inference methods. *Annals of Botany* **122,** 1263–1278.

Savir Y., Noor E., Milo R. & Tlusty T. (2010) Cross-species analysis traces adaptation of Rubisco toward optimality in a low-dimensional landscape. *Proceedings of the National Academy of Sciences of the United States of America* **107,** 3475–3480.

Savolainen V., Fay M.F., Albach D.C., Backlund A., van der Bank M., Cameron K.M., . . . Chase M.W. (2000) Phylogeny of the eudicots: a nearly complete familial analysis based on *rbc*L. *Gene Sequences Kew Bulletin* **55,** 257–309.

Schuettpelz E. & Prier K.M. (2009) Evidence for a Cenozoic radiation of ferns in an angiosperm-dominated canopy. *Proceedings of the National Academy of Sciences of the United States of America* **106,** 11200–11205.

Seemann J.R., Badger M.R. & Berry J.A. (1984) Variations in the specific activity of Ribulose-1,5-bisphosphate carboxylase between species utilizing differing photosynthetic pathways. *Plant Physiology* **74,** 791–794.

Sharwood R.E., von Caemmerer S., Maliga P. & Whitney S.M. (2008) The catalytic properties of hybrid Rubisco comprising tobacco small and sunflower large subunits mirror the kinetically equivalent source Rubiscos and can support tobacco growth. *Plant Physiology* **146,** 83–96.

Soltis D.E., Soltis P.S. & Zanis M.J. (2002) Phylogeny of seed plants based on evidence from eight genes. *American Journal of Botany* **89,** 1670–1681.

Spreitzer R.J. & Salvucci, M.E. (2002) RUBISCO: structure, regulatory interactions, and possibilities for a better enzyme. *Annual Review of Plant Biology* **53,** 449–475.

Tabita F.R. (1999) Microbial ribulose 1,5-bisphosphate carboxylase/oxygenase: a different perspective. *Photosynthesis Research* **60,** 1–28.

Tamura M.N., Yamashita J., Fuse S. & Haraguchi M. (2004) Molecular phylogeny of monocotyledons inferred from combined analysis of plastid *mat*K and *rbc*L gene sequences. *Journal of Plant Research* **117,** 109–120.

Tcherkez G. (2013) Modelling the reaction mechanisms of ribulose-1, 5-bisphosphate carboxylase/oxygenase and consequences for kinetic parameters. *Plant, Cell & Environment* **36,** 1586–1596.

Tcherkez G., Farquhar G.D. & Andrews T.J. (2006) Despite slow catalysis and confused substrate specificity, all ribulose bisphosphate carboxylases may be nearly perfectly optimized. *Proceedings of the National Academy of Sciences of the United States of America* **103,** 7246–7251.

Uemura K., Anwaruzzaman K., Miyachi S. & Yokota A. (1997) Ribulose-1, 5-bisphosphate carboxylase/oxygenase from thermophilic red algae with a strong specificity for CO2 fixation. *Biochemical and Biophysical Research Communications* **233,** 568–571.

Van T.K., Haller W.T. & Bowes G. (1976) Comparison of the photosynthetic characteristics of three submersed aquatic plants. *Plant Physiology* **58,** 761–768.

Von Caemmerer S. (2000) *Biochemical Models of Leaf Photosynthesis*. CSIRO Publishing, Collingwood, Australia.

Walker B., Ariza L.S., Kaines S., Badger M.R. & Cousins A.B. (2013) Temperature response of *in vivo* Rubisco kinetics and mesophyll conductance in *Arabidopsis thaliana*: comparisons to *Nicotiana tabacum*. *Plant, Cell and Environment* **36,** 2108–2119.

Wang M., Kapralov M.V. & Anisimova M. (2011) Coevolution of amino acid residues in the key photosynthetic enzyme Rubisco. *BMC Evolutionary Biology* **11,** 266.

Webb C.O., Ackerly D.D. & Kembel S.W. (2008) Phylocom: software for the analysis of phylogenetic community structure and trait evolution. *Bioinformatics (Oxford, England)* **24,** 2098–2100.

Whitney S.M. & Andrews T.J. (1998) The CO_2/O_2 specificity of single subunit ribulose-bisphosphate carboxylase from the dinoflagellate, *Amphidinium carterae*. *Australian Journal of Plant Physiology* **25,** 131–138.

Whitney S.M., Houtz R.L. & Alonso H. (2011a) Advancing our understanding and capacity to engineer nature's CO2-sequestering enzyme, Rubisco. *Plant Physiology* **155,** 27–35.

Whitney S.M., Sharwood R.E., Orr D., White S.J., Alonso H. & Galmés J. (2011b) Isoleucine 309 acts as a C_4 catalytic switch that increases ribulose-1,5-bisphosphate carboxylase/oxygenase (Rubisco) carboxylation rate in *Flaveria*. *Proceedings of the National Academy of Sciences of the United States of America* **108,** 14688–14693.

Willis K.J. & McElwain J.C. (2002) *The Evolution of Plants*, Oxford University Press, Oxford.

Yang Z. (1997) PAML: a program package for phylogenetic analysis by maximum likelihood. *Computer Applications in the Biosciences* **13,** 555–556.

Yang Z. (2007) PAML 4: phylogenetic analysis by maximum likelihood. *Molecular Biology and Evolution* **24,** 1586–1591.

Yang Z., Wong W.S.W. & Nielsen R. (2005) Bayes empirical Bayes inference of amino acid sites under positive selection. *Molecular Biology and Evolution* **22,** 1107–1118.

Yeoh H.-H., Badger M.R. & Watson L. (1980) Variations in Km-CO_2 of ribulose-1,5-bisphosphate carboxylase among grasses. *Plant Physiology* **66,** 1110–1112.

Yeoh H.-H., Badger M.R. & Watson L. (1981) Variations in kinetic properties of ribulose-1,5-bisphosphate carboxylases among plants. *Plant Physiology* **67,** 1151–1155.

Yokota A. & Canvin D.T. (1985) Ribulose bisphosphate carboxylase/oxygenase content determined with [^{14}C]carboxypentitol bisphosphate in plants and algae. *Plant Physiology* **77,** 735–739.

Young J.N., Rickaby R.E.M., Kapralov M.V. & Filatov D.A. (2012) Adaptive signals in algal Rubisco reveal a history of ancient atmospheric carbon dioxide. *Philosophical Transactions of the Royal Society B: Biological Sciences* **367,** 483–492.

Zarzycki J., Brecht V., Müller M. & Fuchs G. (2009) Identifying the missing steps of the autotrophic 3-hydroxypropionate CO_2 fixation cycle in *Chloroflexus aurantiacus*. *Proceedings of the National Academy of Sciences* **106,** 21317–21322.

Zhu X.G., Portis A.R. & Long S.P. (2004) Would transformation of C_3 crop plants with foreign Rubisco increase productivity? A computational analysis extrapolating from kinetic properties to canopy photosynthesis. *Plant, Cell and Environment* **27,** 155–165.

Zhu X.G., Long S.P. & Ort D.R. (2010) Improving photosynthetic efficiency for greater yield. *Annual Review of Plant Biology* **61,** 235–261.

von Caemmerer S. (2013) Steady-steate models of photosynthetis. *Plant, Cell and Environment* **36,** 1617–1630.

Received 5 February 2014; received in revised form 19 March 2014; accepted for publication 22 March 2014

SUPPORTING INFORMATION

Additional Supporting Information may be found in the online version of this article at the publisher's web-site:

Figure S1. The phylogeny of analysed 28 species based on synonymous positions of the rbcL alignment and

reconstructed using maximum likelihood algorithm. Bootstrap values after 1000 permutations are given above branches.

Table S1. Phylogenetically independent contrast (PIC) correlation coefficients (upper right of the diagonal) and Pearson's correlation coefficients (lower left of the diagonal) between Rubisco content and kinetic parameters of 34 plant species and cultivars. The concentration of total leaf-soluble protein being Rubisco ([Rubisco]/[TSP]), the Michaelis–Menten constants for CO_2 (K_c) and O_2 (K_o), the maximum carboxylation rate (k_{cat}^c) and the carboxylation catalytic efficiency (k_{cat}^c/K_c). Data were log-transformed before independent contrasts and Pearson's correlation. Traits that are significantly correlated are marked: ***$P < 0.005$; **$P < 0.01$; *$P < 0.05$.